EUROPEAN ORGANIZATION FOR NUCLEAR RESEARCH

EXPERIMENTAL RESULTS ON DIFFRACTIVE ONE-PION PRODUCTION AT THE CERN ISR

H. de Kerret, E. Nagy[1], M. Regler[2], W. Schmidt-Parzefall, K.R. Schubert[3] and K. Winter

CERN, Geneva, Switzerland

A. Brandt, H. Dibon, G. Flügge[4], F. Niebergall and P.E. Schumacher

II. Institut für Experimentalphysik, Hamburg, Germany

J.J. Aubert[5], C. Broll[5], G. Coignet[5], J. Favier[5], L. Massonnet[5] and M. Vivargent[5]

Institut de Physique Nucléaire, Orsay, France

W. Bartl, H. Eichinger, Ch. Gottfried and G. Neuhofer

Institut für Hochenergiephysik, Vienna, Austria

ABSTRACT

New experimental results are reported on diffractive dissociation of protons into $(n\pi^+)$ in proton-proton collisions at a centre-of-mass energy of $\sqrt{s}$ = 45 GeV. The data were obtained using the Split-Field-Magnet detector at the CERN Intersecting Storage Rings. We have searched for resonance contributions and found peaks at mass values of 1.5 GeV, 1.65 GeV, and 2.1 GeV. A dip in $d\sigma/dt$ is observed at low t and low mass; it is most pronounced for events with neutrons emitted at 90° in the Gottfried-Jackson frame. The correlation between mass and slope depends strongly on Θ_J. The cross-section of the channel $pp \to pn\pi^+$ is 400 ± 110 μb at $\sqrt{s}$ = 45 GeV, giving an energy dependence of $s^{-0.30\pm0.07}$ for isospin exchange zero in this channel.

Geneva - 25 May 1976

(Submitted to Physics Letters B)

---

1 Visitor from the Central Research Institute for Physics, Budapest, Hungary.

2 Now at Institut für Hochenergiephysik, Vienna, Austria.

3 Now at Institut für Hochenergiephysik, Heidelberg, Germany.

4 Now at DESY, Hamburg, Germany.

5 Now at Laboratoire de Physique des Particules, Annecy, France.

We have investigated the diffractive dissociation of protons into a neutron and a pion using the Split-Field-Magnet detector (SFM) at the CERN Intersecting Storage Rings (ISR). We have obtained data with high statistics on the exclusive reaction:

$$pp \rightarrow p(n\pi^+) \tag{1}$$

over the whole ISR energy range. We report here results [1] at the energy $\sqrt{s}$ = 45 GeV, corresponding to an integrated luminosity of 1.4×10^{35} cm^{-2}. In this letter we shall discuss the production properties of the process and compare them with results at low energy. In the following letter we shall present results on the decay of the $(n\pi^+)$ system.

The SFM detector has been described elsewhere [2]: it contains two forward telescopes equipped with 28 multiwire proportional chambers of 2 mm wire spacing, most of them 1 m high and 2 m wide. Each chamber has a vertical and a horizontal wire plane. The magnetic field is 1.0 T for the energy $\sqrt{s}$ = 45 GeV, resulting in a momentum resolution of $\Delta p/p = \pm 6\%$ for scattered protons. As shown in fig. 1, the detector is complemented by four neutron detectors [3], each of them consisting of a carbon converter followed by two multiwire proportional chambers used to reconstruct the neutron impact. The spatial resolution is ±2.5 mm in each projection for an over-all detection efficiency, due to neutron conversion probability and off-line reconstruction criteria, varying between 3% and 6% with the neutron momentum and its impact position. This detector provides an average $(n\pi^+)$ mass resolution of ±15 MeV (one standard deviation).

Events are selected in three steps; a fast trigger requires at least one charged particle in each telescope, using signals from the proportional chambers, and a neutron conversion signal on one side. A slow trigger with a decision time of about 2 μsec imposes multiplicity conditions and performs a rough track finding using memory levels of groups of 32 wires [4]. This memory level logics reduces the trigger rate by a factor of 20 to 50. Finally, an on-line program filters the neutron counter information.

We have recorded 3.27 million triggers and have processed them with an off-line analysis chain consisting of three programs. A pattern recognition program reconstructs the neutron impact and finds track candidates; a geometrical fit [5] is performed in the magnetic field and the directions and momenta of the charged particles and their vertex are calculated. Finally, a kinematical fit with three constraints (the neutron momentum being unknown) is performed and events corresponding to a confidence level larger than 1% are retained.

Reaction (1) can be described by four variables: the momentum transfer t between the incident and the final proton, the invariant mass m of the $(n\pi^+)$ system, and the polar and azimuthal angles Θ_J and ϕ_J of the neutron in the Gottfried-Jackson system [6]. In order to determine the fourfold differential cross-section

$$\frac{d^4\sigma}{dt\ dm\ d\cos\Theta_J\ d\phi_J},$$

an acceptance correction depending on these four variables must be applied to the data, and they must be multiplied by an over-all normalization factor. The geometrical acceptance of the detector for reaction (1) was calculated using Monte Carlo methods [7]. The inhomogeneity of the detector implies the need to calculate the acceptance for a large number of small intervals in the four variables, resulting in a four-dimensional table of 38640 cells. A selection of usable phase space was made, eliminating a few regions of too low acceptance. The limits of the selected phase space depend on the value of cos Θ_J *1.

After these cuts we are left with 73,870 events. The absolute normalization was obtained by collecting monitor counts using a scintillation counter system (shown in fig. 1) calibrated with the Van der Meer method [8]. A check of this monitor was performed using elastic events taken simultaneously [9]. An over-all scale uncertainty of ±20% due to systematical effects was estimated*2. No background was subtracted; a study of the momentum unbalance in various parts of the phase space has shown that the contamination with background is smaller than 10% everywhere.

The $(n\pi^+)$ mass spectrum obtained after integration over the other variables is shown in fig. 2a. It displays the well-known low-mass enhancement, peaking at approximately 1.35 GeV and on top of it, two resonance-like structures at 1.5 and 1.65 GeV. We have compared this mass spectrum obtained at 1000 GeV/c equivalent incident momentum with the one observed for the same final state and event selection in 14 GeV/c $\pi^{\pm}p$ interactions [10] and conclude that they are compatible. In order to enhance weak resonant signals we have investigated the distribution in momentum transfer t_2 between the dissociating proton and the neutron which is expected to be different for resonant and non-resonant contributions. A resonance can decay transversely, thus leading to high values of $|t_2|$; the larger the mass of a resonance, the larger $|t_2|$ can be. For non-resonant background, one may

---

*1 The detector has the following acceptance:
for $-0.9 < \cos\Theta_J < -0.3$: $1.3 < m < 2$ GeV and $0.1 < |t| < 1.2$ GeV^2
for $-0.3 < \cos\Theta_J < +1$: $1.15 < m < 2.4$ GeV and $0.05 < |t| < 1.2$ GeV^2
The region $\cos\Theta_J < -0.9$ is not accessible in this experiment.

*2 This is a scale uncertainty and consequently does not appear on the figures, except for the cross-section. On all others the error bars are purely statistical.

reasonably assume an exponential decrease with t_2 with a slope of 4 or 5 GeV^{-2}, resulting in a strong suppression at large $|t_2|$ values; a Deck-type non-resonant background, for example, would also give a rapid decrease with increasing $|t_2|$. The effect of selecting events by a $|t_2|$ cut can be observed in fig. 2b, where the two resonant peaks are enhanced compared to the non-resonant part. An additional cut on the decay angle Θ_J has been useful to attenuate the tail of lower mass resonances when looking for high-mass signals. For events with forward-produced neutrons a resonance-like signal is observed at $\sim$ 2.1 GeV in figs. 2c and 2d. The dashed lines indicate the onset of the acceptance region for forward-produced N^*'s.

In order to study the t-dependence of the cross-section down to small $|t|$ values*1 we select events with $\cos \Theta_J > -0.3$. Integrating over $\cos \Theta_J$ and ϕ_J for various mass bands and fitting the small $|t|$ region with an exponential one finds the well-known mass-slope correlation. The results are given in table 1, showing a variation of the slope from approximately 20 GeV^{-2} near threshold to 4 GeV^{-2} in the high-mass region, as was found at lower energies [11]. At low-mass values we observe a dip structure in the $|t|$ region from 0.15 to 0.25 GeV^2. Both this structure and the correlation can be interpreted [12] in terms of a peripheral profile in impact parameter space and increasing contributions of helicity flip amplitudes with increasing mass.

A new, hitherto unpredicted feature of these data is the correlation between production and decay of the $(n\pi^+)$ system. We observe a strong variation of the slope parameter with the Gottfried-Jackson angle Θ_J and dominance of the dip of $d\sigma/dt$ at low $|t|$ values for $\Theta_J \sim 90°$. The dependence of $d\sigma/dt$ on the invariant mass in the interval $-0.3 < \cos \Theta_J < 0.3$ is shown in fig. 3a. A dip in the cross-section occurs at $-t = 0.14$ GeV^2 for $1.15 < m < 1.20$ GeV; its position is shifting with the mass to $-t = 0.25$ GeV^2 for $1.35 < m < 1.40$ GeV^2, where it presents itself as a change of slope. The slopes of an exponential parametrization of $d\sigma/dt$ in fig. 3a are given in table 2. The dependence of this dip structure on Θ_J is shown in fig. 3b for one mass interval, $1.30 < m < 1.35$ GeV. At small values of Θ_J the dip structure has vanished and the data are well described by a single slope. The sensitivity in the backward hemisphere of Θ_J is somewhat limited owing to an acceptance cut-off*1 at $|t| > 0.1$ GeV^2 and lack of statistics; nevertheless, it can be noted that there is no pronounced dip as for $\Theta_J \sim 90°$. The slopes of an exponential representation of $d\sigma/dt$ in fig. 3b are given in table 2 together with the $|t|$ intervals of the fit.

The mass-slope correlation is shown in fig. 4a for two intervals of Θ_J. We note an increase of slope for $\Theta_J \sim 90°$ outside the resonance region $1.5 < m < 1.8$ GeV, both for small and for large masses. The strong variation of the slope with Θ_J in a single mass interval, $1.30 < m < 1.35$ GeV corresponding to fig. 3b, is shown in fig. 4b. We note that a small slope value is occurring even at small mass if $\Theta_J \sim 0°$.

The results of a model calculation*3 for non-resonant contributions, incorporating a double-peripheral mechanism, is also shown in fig. 4. This mechanism does indeed give a similar trend of correlation between production and decay.

To obtain the integrated channel cross-section we have extrapolated $d\sigma/dt$ to $t = 0$ and accounted for the missing parts of the phase space. We find [13]

$$\sigma(pp \to pn\pi^+) = 400 \pm 110\ \mu b \qquad \text{at } \sqrt{s} = 45\ \text{GeV} .$$

The error contains an estimate of the scale uncertainty of ±20% and of the extrapolation uncertainty. Neglecting contributions due to the exchange of isospin 1 in the t channel [13], one obtains the cross-section for isospin 0 exchange from the relation

$$\sigma[NN \to N(N\pi)]_{I_{ex}=0} = \frac{3}{2}\,\sigma[pp \to p(n\pi^+)] .$$

Comparing*4 with lower energy data [14], we find that the isospin 0 exchange cross-section is compatible with a simple power law dependence:

$$\sigma = a \cdot s^{-0.30 \pm 0.07} .$$

We have obtained the cross-section for the 1.65 GeV peak by subtracting from the mass spectrum the non-resonant part estimated with a model [7]. Extrapolating to $t = 0$ and allowing for the other decay modes, assuming we observe the $N^*(1680)$, yields the following estimate:

$$\sigma(pp \to pN^*_{1680}) = 170 \pm 60\ \mu b .$$

This value, in contrast with a preceding ISR result [15], is in agreement with a simple power law extrapolation of lower energy data, $\sigma \propto s^{-n}$, with $n = 0.34 \pm 0.06$ [16], compatible with that of the isospin 0 exchange cross-section.

To summarize, the $(n\pi^+)$ mass spectrum of the diffractive process $pp \to p(n\pi^+)$ is independent of the energy from $s = 15\ \text{GeV}^2$ to $2000\ \text{GeV}^2$. The cross-section of the dominant isospin $I = 0$ exchange part of this exclusive channel is decreasing as $s^{-0.30 \pm 0.07}$, whereas the inclusive, total diffraction cross-section

---

*3 The matrix element used is described in the following letter.

*4 To be compared with ours, the lower energy results have to be multiplied by two in order to account for dissociation of either proton.

seems to be approximately constant [17]. Owing to the large statistics of this experiment, we have observed some new features. In a selective search for resonances we have found a peak at m = 2.1 GeV. A dip in $d\sigma/dt$ is observed at low t and low mass; it is most pronounced at decay angles $\Theta_J \sim 90°$. Also the slope of $d\sigma/dt$ is found to be strongly correlated with the decay angle Θ_J; the well-known mass-slope correlation is largely due to this correlation and a strong dependence of the angular distribution in Θ_J on mass. This correlation between production and decay can be qualitatively described by a double-peripheral mechanism.

Acknowledgements

We wish to thank W. Wilmsen for his contribution to developing and building the slow trigger electronics, and A. King, N. Mehlführer, M. Moynot, M. Pupunat and J.P. Reuter for their technical assistance. We gratefully acknowledge the support and the work of the SFM Detector Group. We thank M. Metcalf, F. Ranjard and Z. Sekera for their assistance in programming, and F. Blin and J. Guerin for their work in data processing. The group from the University of Hamburg wishes to acknowledge financial support from the Bundesministerium für Forschung und Technologie, Bonn, Germany.

REFERENCES

[1] Preliminary results from this experiment at $\sqrt{s}$ = 53 GeV have been given by E. Nagy, M. Regler, W. Schmidt-Parzefall, K. Winter, A. Brandt, G. Flügge, F. Niebergall, K.R. Schubert, P.E. Schumacher, C. Broll, G. Coignet, J. Favier, L. Massonnet, M. Vivargent, W. Bartl, H. Dibon, Ch. Gottfried and G. Neuhofer, Proc. 17th Internat. Conf. on High-Energy Physics, London, 1974 (Rutherford Lab., Chilton, Didcot, 1974), p. I-13.

[2] R. Bouclier, G. Charpak, E. Chesi, L. Dumps, H.G. Fischer, H.J. Hilke, P.G. Innocenti, G. Maurin, A. Minten, L. Naumann, F. Piuz, J.C. Santiard and O. Ullaland, Nucl. Instrum. Methods 115 (1974) 235.

[3] J.J. Aubert, C. Broll, G. Coignet, J. Favier, L. Massonnet, D.B. Smith, M. Vivargent and H. Dibon, Proc. 5th Internat. Conf. on Instrumentation for High-Energy Physics, Frascati, 1973 (Lab. Naz. del CNEN, Frascati, 1973), p. 410.

[4] A. Brandt, H. Dibon, G. Flügge, F. Niebergall, K.R. Schubert, P.E. Schumacher and W. Wilmsen, Nucl. Instrum. Methods 126 (1975) 519.

[5] M. Metcalf, M. Regler and C. Broll, CERN 73-2 (1973).
J.J. Aubert and C. Broll, Nucl. Instrum. Methods 120 (1974) 137.

[6] K. Gottfried and J.D. Jackson, Nuovo Cimento 33 (1964) 309.

[7] A detailed account of the analysis and complementary physics results can be found *in* C. Broll, Thèse, Université de Paris-Orsay (1975).

[8] S. Van der Meer, CERN Internal Report ISR-PO/68-31.

[9] N. Kwak, E. Lohrmann, E. Nagy, M. Regler, W. Schmidt-Parzefall, K.R. Schubert, K. Winter, A. Brandt, H. Dibon, G. Flügge, F. Niebergall, P.E. Schumacher, J.J. Aubert, C. Broll, G. Coignet, J. Favier, L. Massonnet, M. Vivargent, W. Bartl, H. Eichinger, Ch. Gottfried and G. Neuhofer, Phys. Letters 58B (1975) 233.

[10] J. Ballam, J. Carroll, G. Chadwick, P. Herquet, D. Linglin, K. Moffeit, V. Davidson, A. Dzierba, A. Firestone, W. Ford, R. Gomez, R. Ely, D. Grether and P. Oddone, SLAC-PUB 1657 (1975).

[11] J. Biel, E. Bleser, T. Ferbel, D. Freytag, B. Gobbi, L. Kenah, J. Rosen, R. Ruchti, P. Slattery and D. Underwood, Phys. Rev. Letters 36 (1976) 504,
K. Böckmann, H.G. Heilmann, U. Idschok, P. Kobe, F. Selonke, V. Blobel, H. Fesefeldt, B. Hellwig, D. Mönkemeyer, H. Franz, D. Freund and W. Schrankel, Nucl. Phys. B81 (1974) 45.
See also ref. 7 for a detailed comparison.

[12] G.L. Kane, Acta Phys. Polon. B3 (1972) 845.
H.I. Miettinen, Proc. IXth Rencontre de Moriond, Méribel-les-Allues, 1974 (ed. J. Tran Thanh Van).
S. Humble, Nucl. Phys. B76 (1974) 137.

[13] $\sigma(pp \to pn\pi^+)$ is nearly equal to $\sigma(pp \to p(n\pi^+))$ which was actually measured, since the cross-section of the reaction $pp \to n(p\pi^+)$ is less than 1 μb as measured by N. Kwak, E. Nagy, M. Regler, W. Schmidt-Parzefall, K.R. Schubert, K. Winter, A. Brandt, H. Dibon, G. Flügge, F. Niebergall, P.E. Schumacher, J.J. Aubert, C. Broll, G. Coignet, J. Favier, L. Massonnet, M. Vivargent, W. Bartl, H. Eichinger, Ch. Gottfried and G. Neuhofer, A measurement of the cross-section of the reaction $pp \to n\Delta^{++}(1232)$ at ISR energies (Phys. Letters B, in the press).

[14] E. Dahl-Jensen, I. Dahl-Jensen, J.D. Hansen, R. Möllerud, J. Mäkela, M. Pimiä, E. Sundell, V. Bakken, J. Haldorsen, T. Jacobsen, G. Skjevling, G. Ekspong, H. Johansson, P. Lundborg and B. Sellden, Nucl. Phys. B87 (1975) 426.

[15] R. Webb, G. Trilling, V. Telegdi, P. Strolin, B. Shen, P. Schlein, J. Rander, B. Naroska, T. Meyer, W. Marsh, W. Lockman, J. Layter, A. Kernan, M. Hansroul, S.Y. Fung, H. Foeth, R. Ellis, A. Derevshikov, M. Bozzo, A. Böhm and L. Baksay, Phys. Letters 55B (1975) 331.

[16] R.M. Edelstein, R.A. Carrigan Jr., N.C. Hien, T.J. McMahon, I. Nadelhaft, E.W. Anderson, E.J. Bleser, G.B. Collins, T. Fujii, J. Menes and F. Turkot, Phys. Rev. D 5 (1972) 1073.

[17] See, for example, R.D. Schamberger Jr., J. Lee-Franzini, R. McCarthy, S. Childress and P. Franzini, Phys. Rev. Letters 34 (1975) 1121 and M.G. Albrow, A. Bagchus, D.P. Barber, P. Benz, A. Bogaerts, B. Bosñjakovič, J.R. Brooks, C.Y. Chang, A.B. Clegg, F.C. Erné, C.N.P. Gee, P. Kooijman, D.H. Locke, F.K. Loebinger, N.A. McCubbin, P.G. Murphy, D. Radojicic, A. Rudge, J.C. Sens, A.L. Sessoms, J. Singh, D. Stork and J. Timmer, submitted to Nucl. Phys. B, January 1976.

Table 1

Slope values b of an exponential representation of $d\sigma/dt$ and the $|t|$ intervals of the fit as a function of mass and for two intervals of $\cos\Theta_J$

Mass interval (GeV)	Slope b for $\cos\Theta_J > -0.3$ (GeV^{-2})	$\|t\|$ interval for fitting (GeV^2)	Slope b for $-0.3 < \cos\Theta_J < +0.3$ (GeV^{-2})	$\|t\|$ interval for fitting (GeV^2)
1.15-1.2	19.6 ± 1.6	< 0.15	26.1 ± 4.6	< 0.13
1.2 -1.25	17.2 ± 0.8	< 0.15	24.8 ± 2.3	< 0.15
1.25-1.30			26.3 ± 2.2	< 0.15
1.30-1.35	14.6 ± 0.7	< 0.15	24.2 ± 1.4	< 0.21
1.35-1.40			22.2 ± 1.6	< 0.21
1.40-1.50	10.2 ± 0.7	< 0.15	16.6 ± 1.1	< 0.21
1.50-1.60	6.3 ± 0.2	< 0.45	8.7 ± 1.3	< 0.21
1.60-1.70	6.1 ± 0.2	< 0.45	6.1 ± 0.8	< 0.29
1.70-1.80	5.7 ± 0.2	< 0.45	5.4 ± 0.55	< 0.45
1.8 -2.0	4.4 ± 0.2	< 0.45	7.1 ± 0.6	< 0.45
2.0 -2.4	4.0 ± 0.3	< 0.45	6.9 ± 0.6	< 0.45

Table 2

Slope values of $d\sigma/dt$ as a function of $\cos\Theta_J$ in the region $1.3 < m < 1.35$ GeV

$\cos\Theta_J$ interval	$\|t\|$ interval for fitting (GeV^2)	Slope and fit error (GeV^{-2})
-0.9 - -0.3	0.1 - 0.21	24.7 ± 5
-0.3 - +0.3	0.05 - 0.21	24.2 ± 1.4
+0.3 - +0.6	0.05 - 0.21	14.6 ± 1
+0.6 - +0.8	0.05 - 0.21	11.2 ± 1
+0.8 - 1.0	0.05 - 0.21	4.7 ± 0.8

Figure captions

Fig. 1 : Schematic view of the SFM detector. N_1, N_2, N_3, and N_4 are neutron impact detectors triggered by a coincidence between scintillators $\bar{A}_i B_i C_i$ (i = 1, 2, 3, 4). T1 and T2 are monitor counters.

Fig. 2 : a) Integrated spectrum of invariant mass. The cross-hatched region corresponds to a restricted phase space*1.

b) Mass spectrum after a cut on $|t_2|$. $|t_2|$ is the squared momentum transfer between the dissociating proton and the neutron.

c) and d) Mass spectra after cuts on $|t_2|$ and the Gottfried-Jackson angle Θ_J. The dashed lines indicate the threshold for forward-produced N^*.

Fig. 3 : a) $d\sigma/dt$ as a function of momentum transfer t in various mass regions of the $(n\pi^+)$ system for $-0.3 < \cos\Theta_J < 0.3$.

b) $d\sigma/dt$ in various regions of $\cos\Theta_J$ for the mass interval $1.3 < m < 1.35$ GeV.

Fig. 4 : a) Slope value b of an exponential representation of $d\sigma/dt$ as a function of mass for two intervals of $\cos\Theta_J$.

b) Slope value b as a function of $\cos\Theta_J$ for $1.3 < m < 1.35$ GeV.

The continuous lines represent the result of a model calculation of non-resonant background. Values of b and the intervals of the fit are given in tables 1 and 2.

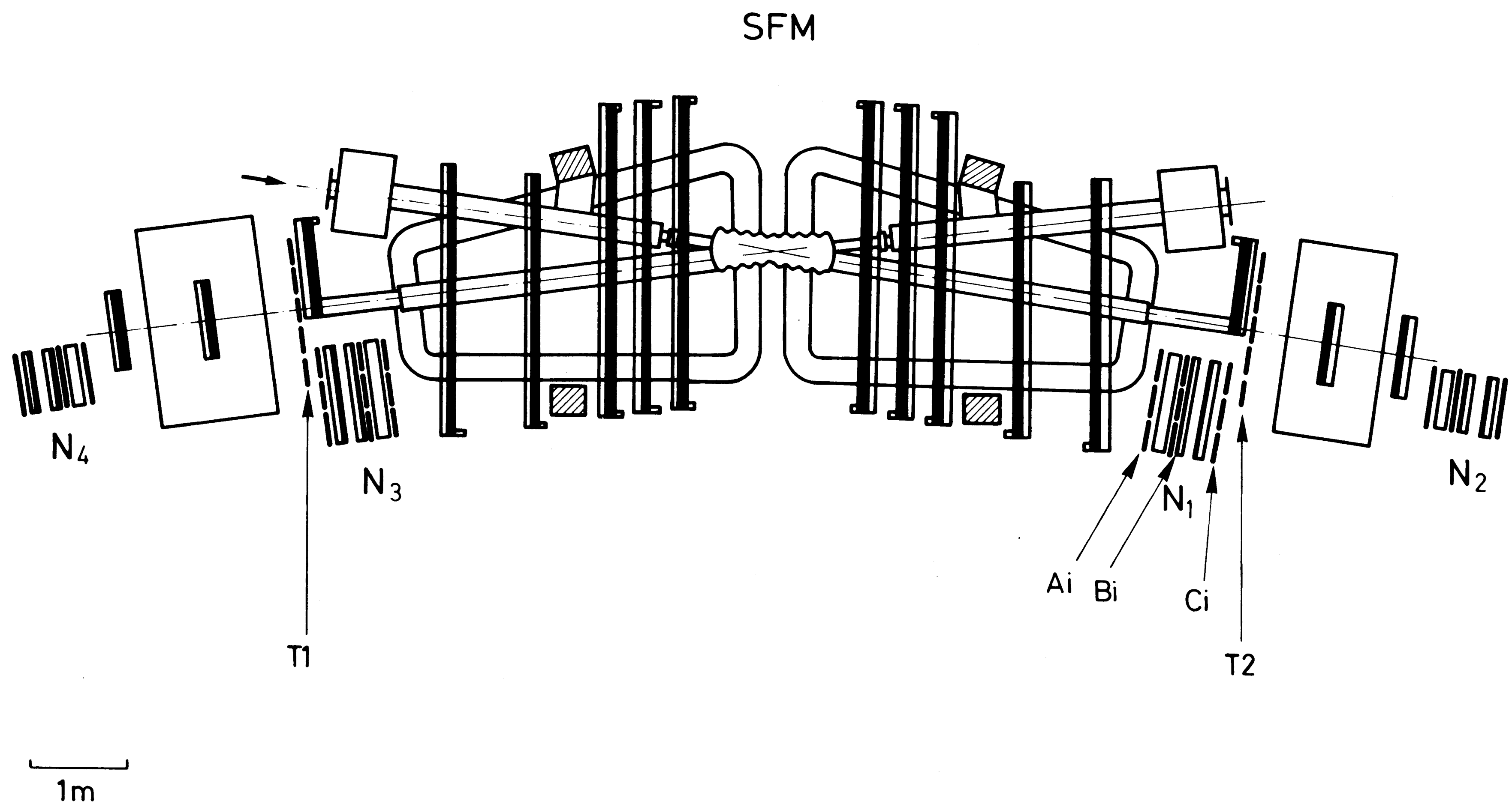

Fig. 1

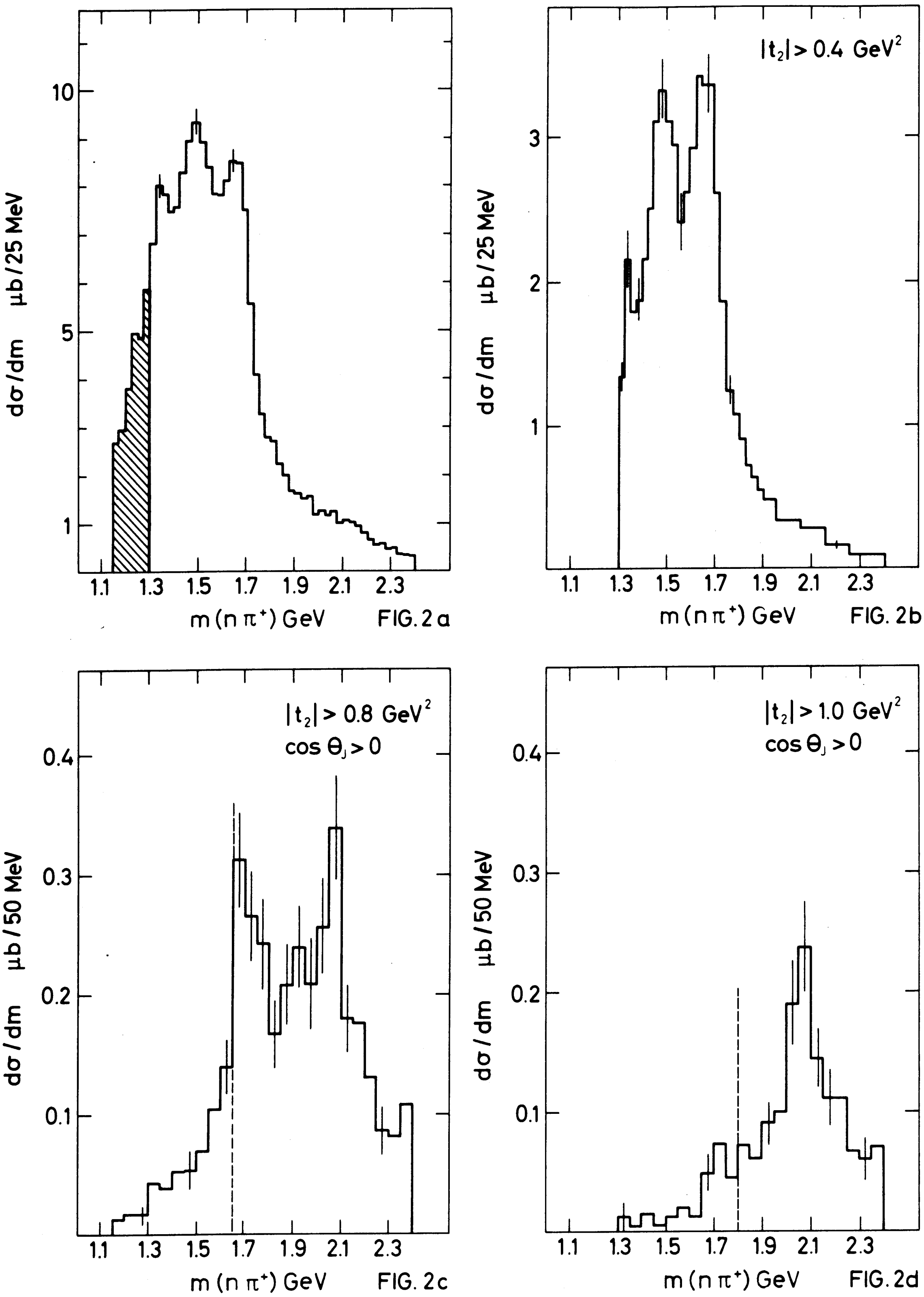
dσ/dm μb/25 MeV
10
5
1
1.1 1.3 1.5 1.7 1.9 2.1 2.3
m(nπ⁺) GeV
FIG. 2a
|t₂| > 0.4 GeV²
dσ/dm μb/25 MeV
3
2
1
1.1 1.3 1.5 1.7 1.9 2.1 2.3
m(nπ⁺) GeV
FIG. 2b
|t₂| > 0.8 GeV²
cos θ_J > 0
dσ/dm μb/50 MeV
0.4
0.3
0.2
0.1
1.1 1.3 1.5 1.7 1.9 2.1 2.3
m(nπ⁺) GeV
FIG. 2c
|t₂| > 1.0 GeV²
cos θ_J > 0
dσ/dm μb/50 MeV
0.4
0.3
0.2
0.1
1.1 1.3 1.5 1.7 1.9 2.1 2.3
m(nπ⁺) GeV
FIG. 2d

Fig. 2

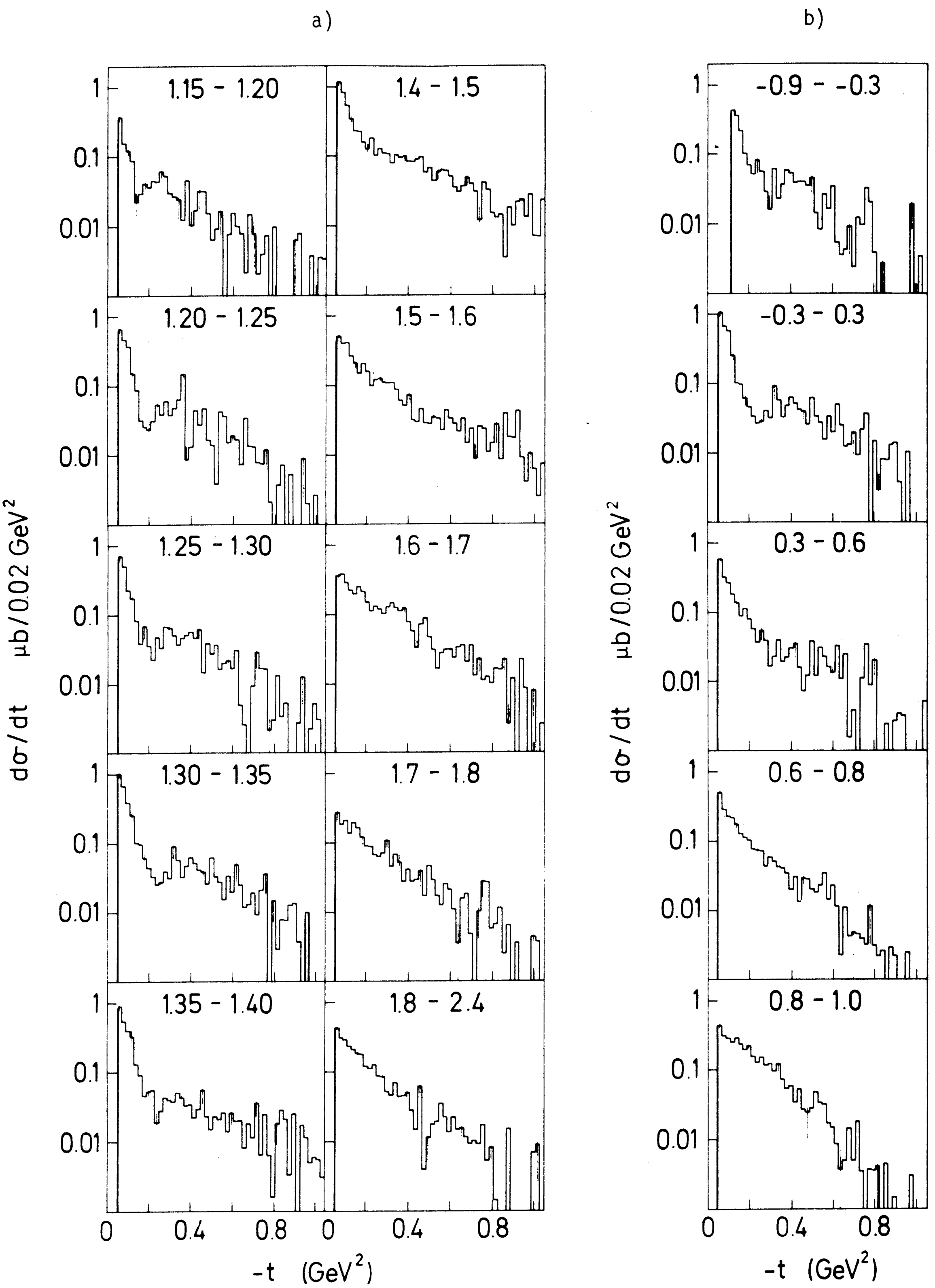
a)
b)
1.15 - 1.20
1.4 - 1.5
1.20 - 1.25
1.5 - 1.6
1.25 - 1.30
1.6 - 1.7
1.30 - 1.35
1.7 - 1.8
1.35 - 1.40
1.8 - 2.4
-0.9 - -0.3
-0.3 - 0.3
0.3 - 0.6
0.6 - 0.8
0.8 - 1.0
1
0.1
0.01
dσ/dt μb/0.02 GeV²
0
0.4
0.8
-t (GeV²)

Fig. 3

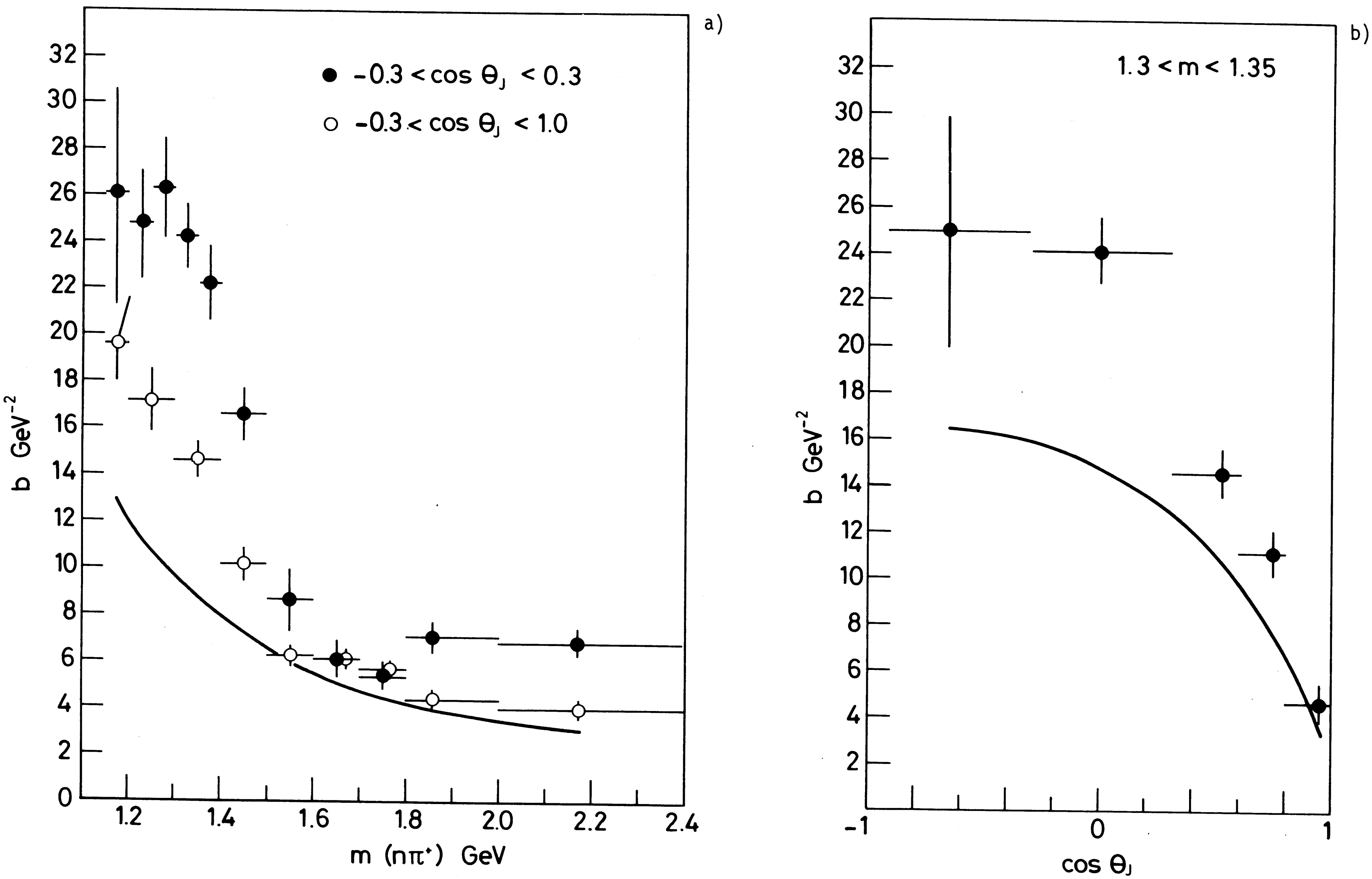

Fig. 4